PHYSICAL REVIEW A **90**, 062126 (2014)

Uncertainty formulations for multislit interferometry

Johannes C. G. Biniok*
University of York, York YO10 5DD, United Kingdom
(Received 29 September 2014; published 22 December 2014)

In the context of (far-field) multislit interferometry we investigate the utility of two formulations of uncertainty in accounting for the complementarity of spatial localization and fringe width. We begin with a characterization of the relevant observables and general considerations regarding the suitability of different types of measures. The detailed analysis shows that both of the discussed uncertainty formulations yield qualitatively similar results, confirming that they correctly capture the relevant tradeoff. One approach, based on an idea of Aharonov and co-workers, is intuitively appealing and relies on a modification of the Heisenberg uncertainty relation. The other approach, developed by Uffink and Hilgevoord for single- and double-slit experiments, is readily applied to multislits. However, it is found that one of the underlying concepts requires generalization and that the choice of the parameters requires more consideration than was known.

DOI: 10.1103/PhysRevA.90.062126 PACS number(s): 03.65.−w

I. INTRODUCTION

Multislit experiments are central to the foundational considerations in quantum mechanics since the Bohr-Einstein debate. Despite that, a number of open questions remain regarding the suitability of the various uncertainty formulations proposed to address the inadequacy of the Heisenberg uncertainty relation in this context. Uncertainty relations are intended to express the qualitative understanding about microscopic systems that is embodied in the principle of uncertainty. However, a particular formulation of uncertainty comes with a scope of validity and might not capture the relevant tradeoff in a given situation. For instance, take the so-called Heisenberg relation

$$\Delta(Q,\Psi)\,\Delta(P,\Psi) \geqslant 1/2, \tag{1}$$

relating the standard deviation of position and of momentum in state Ψ in the form of a tradeoff relation. (We are using units such that $\hbar = 1$.) The fact that the Heisenberg relation fails at quantifying the uncertainty of quantum states prepared in multislit experiments is well documented. The particular cause of this failure, however, is not agreed upon: Although it was suggested that the Heisenberg relation is unsuitable because of the inadequacy of standard deviations, it is that momentum is not the correct observable to consider. In fact, we show here that a Heisenberg-type uncertainty relation yields the same qualitative results—by virtue of appropriately chosen observables—as an alternative formulation of uncertainty, which does without standard deviations.

While experiments suggest that the spatial localization at the aperture mask and the fringe property of the interference pattern constitute a pair of incompatible observables, whose relationship is described by an uncertainty tradeoff, the precise character of this relationship or the particular form of the relevant observables is not obvious. We address both these matters at a general level. This results in a better understanding of the significance of the envelope to the interference pattern and the functions governing its fine structure. Thus we can address the suitability of different kinds of measures at an equally general level, concluding that measures of fringe width capture the relevant observable in the context of multislit experiments. In this way, the general discussion also serves as a justification of the particular choice of uncertainty formulations discussed here, as each employs a measure of fringe width. Furthermore, the insights obtained are found valuable for the example applications considered.

We then proceed to address the failure of the Heisenberg relation. Two courses of action are available for obtaining a correct expression of the uncertainty principle for applications in multislit interferometry: The already established Heisenberg relation could be modified or replaced. Both options are discussed and compared. We explore a modification based on work by Aharonov, Pendleton, and Peterson (APP), who proposed an uncertainty formulation by way of a heuristic argument presented in Ref. [1]. Also, we investigate the alternative relation that was derived by Uffink and Hilgevoord (UH) in their extensive study of single- and double-slit experiments reported in Ref. [2] and related work. *Prima facie* both formulations of uncertainty appear more suitable than the Heisenberg relation for two reasons. First, two distinct measures are used, reflecting the two different properties that are measured—that being the spatial localization on the one hand and the fringe width on the other. Second, both formulations of uncertainty reflect the structure observed in multislit experiments.

II. GENERAL CONSIDERATIONS

From experimental observation it was concluded that the particular illumination of the aperture mask is related to the character of the fringes seen on a distant detection screen. The change in the interference pattern that results from illuminating more slits suggests that the spatial localization (related to the number of illuminated slits) and the fringe property (related to the appearance and shape of the fringes) constitute a pair of incompatible observables, whose relationship is described by an uncertainty tradeoff. The precise character of this relationship or the particular form of the relevant observables, however, is not obvious. For instance, the fringe property could be expressed using a measure of fringe *width* (two examples of which are discussed below in detail) or fringe *contrast* (also referred to as fringe visibility). The latter is particularly

*jcgb500@york.ac.uk

common in the context of Mach-Zehnder interferometry. These two measures are, however, not equally suitable for a description of multislit experiments.

For the present, let us consider experiments with uniformly illuminated aperture masks of 2^d slits, where d can be any non-negative integer. These setups prepare quantum states ψ_d, whose momentum-space representation $\widehat{\psi}_d(k)$ can be expressed in terms of two functions $\widehat{g}_d(k)$ and $\widehat{f}_d(k)$,

$$\widehat{\psi}_d(k) \propto \widehat{g}_d(k)\, \widehat{f}_d(k), \tag{2}$$

up to some normalization factor. The function $\widehat{g}_d(k)$ describes an envelope; it is referred to as the effective envelope. The function $\widehat{f}_d(k)$ describes the fringe property, i.e., the fine structure of the momentum-space wave function. In previous work [3], a recursive relationship between the wave functions was discussed,

$$\widehat{\psi}_d(k) \propto \widehat{\psi}_{d-1}(k) \cos, \tag{3}$$

arguing that Eqs. (2) and (3) should be identified, giving

$$\widehat{g}_d(k) = \widehat{\psi}_{d-1}(k), \tag{4}$$

$$\widehat{f}_d(k) = \cos. \tag{5}$$

According to Eq. (5), the fine structure of the momentum-space wave function $\widehat{\psi}_d(k)$ is determined by a simple cosine. In fact, this single cosine is all that differentiates $\widehat{\psi}_d(k)$ from $\widehat{\psi}_{d-1}(k)$. As this cosine does not change the overall localization property of the interference pattern, $\widehat{\psi}_d(k)$ shares its localization property with $\widehat{\psi}_{d-1}(k)$. Applying this argument repeatedly, we conclude that the localization property of $\widehat{\psi}_d(k)$ is determined by $\widehat{\psi}_0(k)$.

The quantum state ψ_0 is prepared through illumination of a single slit. However, diffraction is independent of interference, while the present investigation is about superposition states and the resulting interference phenomena. The given choice of aperture, which implies the particular form of $\psi_0(x)$, determines the overall localization properties of the various $\widehat{\psi}_d(k)$ in the form of an envelope $\widehat{\psi}_0(k)$. We refer to $\widehat{\psi}_0(k)$ as the fundamental envelope. While the fundamental envelope is, in general, only part of the effective envelope, it is qualitatively distinct in that it depends on diffraction. Accordingly, a measure of the fringe property should not depend on the fundamental envelope. In fact, there should not be any dependence on the effective envelope, but only dependence on the function actually determining the fine structure of the momentum-space wave function, i.e., Eq. (5). Note that any measure of fringe contrast necessarily has this unwanted dependence.

It follows naturally that the particular wave function chosen for modeling the quantum state prepared by a single slit is not important. Typically, the wave function prepared by a single slit is modeled using a rectangular function

$$\psi_0(x) = \mathrm{rec}_a(x),$$

of width a; see Eq. (19) for a formal introduction of rec_a. This choice is often rejected on the basis of the diverging standard deviation of momentum, i.e., $\Delta(P, \psi_0) = \infty$. However, as we argued, this function is not part of the relevant observable. Hence the concern regarding the diverging standard deviation is unnecessarily restrictive in the given context, and only important when (also) considering single-slit diffraction.

III. UNCERTAINTY BASED ON THE APP MODEL

This formulation of uncertainty is based on a modification of the Heisenberg relation (1). It follows from the realization that the observables of multislit interferometry are not Q and P, but rather a discretized spatial localization (related to the number of illuminated slits) and the width of single fringes rather than the width of the entire momentum distribution. A detailed derivation of this uncertainty formulation was provided in previous work [3]. Here only the necessary definitions are provided in order to use this uncertainty formulation and the interested reader is referred to the earlier discussion.

The relevant observables are obtained using the following decomposition of Q and P:

$$Q = Q_{\mathrm{mod}} + Q_T, \tag{6}$$

$$P = P_{\mathrm{mod}}(n) + P_K(n), \tag{7}$$

where Q is decomposed into a T-periodic part Q_{mod} and a remainder Q_T, and P into a K_n-periodic part $P_{\mathrm{mod}}(n)$ with remainder $P_K(n)$. We use the following abbreviations:

$$K = 2\pi/T, \tag{8}$$

$$K_n = 2\pi/(nT). \tag{9}$$

The abstract quantity n is used to characterize interference wave functions below. The periodic operators are defined in terms of T and K_n,

$$Q_{\mathrm{mod}} = Q \mod T, \tag{10}$$

$$P_{\mathrm{mod}}(n) = (P + K_n/2 \mod K_n) - K_n/2\,. \tag{11}$$

The definitions of the operators Q_T and $P_K(n)$ follow from Eqs. (6) and (7). For wave functions $\widehat{\Psi}(k)$ that vanish periodically,

$$\widehat{\Psi}((j + 1/2)K_n) = 0 \quad \text{for each } j \in \mathbb{Z} \tag{12}$$

(see Ref. [3] regarding this restriction), we have

$$\Delta(Q_T, \Psi)\Delta(P_{\mathrm{mod}}(n), \Psi) \geqslant \tfrac{1}{2}. \tag{13}$$

This is the first uncertainty relation we wish to discuss. Illustrations of Q_T and $P_{\mathrm{mod}}(n)$ are displayed in Fig. 1. Although it may seem like a formidable task to compute the standard deviations of the operators Q_T and $P_{\mathrm{mod}}(n)$ with complicated wave functions, we are going to find that this decomposition actually leads to marvellous simplifications for the considered quantum states, and to intuitively satisfying results.

IV. UNCERTAINTY AS FORMULATED BY UH

In their extensive investigation of uncertainty in the context of single- and double-slit experiments, UH define two measures to express uncertainty [2]. They define the overall width $\Omega_N(\Psi)$ of a normalized wave function Ψ and the mean fringe width $\omega_M(\Psi)$ (in momentum space). They proceed to

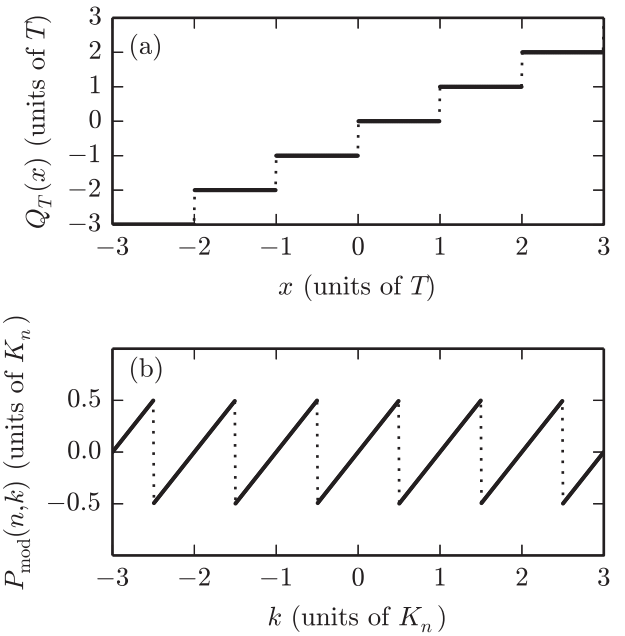

FIG. 1. In (a) Q_T is depicted in position space; it is defined indirectly through Eqs. (6) and (10), whereas (b) illustrates the operator $P_{\mathrm{mod}}(n)$, as defined in Eq. (11), in momentum space as a function of k.

show that an uncertainty relation exists for these quantities, expressing a tradeoff between spatial localization on the one hand, and fine structure in momentum space on the other: The product of $\Omega_N(\Psi)$ and $\omega_M(\Psi)$ is bounded from below. The same analysis applies independently to $\widehat{\Psi}$ (formally obtained by exchanging Ψ for $\widehat{\Psi}$), and hence $\Omega_N(\widehat{\Psi})\,\omega_M(\widehat{\Psi})$ is bounded from below as well. However, we focus on Ψ in our present investigation.

The overall width $\Omega_N(\Psi)$ of a quantum state Ψ is the smallest interval that contains probability N:

$$\Omega_N(\Psi) = \min\left\{|p_1 - p_2| : \int_{p_1}^{p_2} |\Psi(x)|^2 dx = N\right\}. \quad (14)$$

The parameter N is a number less than 1, although chosen close to 1. Note that the value of the overall width necessarily reflects the discreteness of the aperture mask. In the analysis below, particularly of aperture masks with a small number of illuminated slits, this is going to lead to notable discontinuous jumps of the overall width.

The fine structure of $\widehat{\Psi}$ is quantified through the mean fringe width $\omega_M(\Psi)$, which is the smallest shift such that the inner product of $\widehat{\Psi}(k)$ and the shifted $\widehat{\Psi}(k-s)$ is associated with a value M:

$$\omega_M(\Psi) = \min\left\{s : \left|\int_{-\infty}^{\infty} \widehat{\Psi}^*(k)\,\widehat{\Psi}(k-s)dk\right| = M\right\}. \quad (15)$$

The parameter M is chosen smaller than N; see Eq. (18) below. This measure is conceptually rather different; it quantifies how much the momentum-space wave function $\widehat{\Psi}(k)$ deviates from precise values of momentum: $\omega_M(\Psi)$ is not sensitive to the number of momentum peaks, but to how sharp they are. Similar approaches to quantifying uncertainty are also found in other work; for example Ref. [4].

For a normalized quantum state Ψ, the following uncertainty relation, derived and proved by Uffink and Hilgevoord [2], gives a lower bound to the overall width $\Omega_N(\Psi)$ and the mean fringe width $\omega_M(\Psi)$:

$$\Omega_N(\Psi)\,\omega_M(\Psi) \geqslant 2\arccos\left(\frac{M+1}{N} - 1\right), \quad (16)$$

with the following two conditions required:

$$M^2 + N^2 \geqslant 1, \quad (17)$$

$$M \leqslant 2N - 1. \quad (18)$$

Each of the acceptable pairs (N,M) yields another acceptable value for the uncertainty product. While UH found that the exact choice of N and M was not important (for the applications they considered), we arrived at a different conclusion, which is detailed in the analysis below. There are, however, certain qualitative results that indeed might not depend on N or M. For example, the exact choice of M is entirely irrelevant for an analysis of the double-slit state so long as N is chosen very close to unity. Then, the uncertainty is approximately equal to the lower bound for any M (strictly true for $N = 1$).

UH state that (in adapted notation) "$\omega_M(\Psi)$ and $\Omega_N(\Psi)$ are governed by the slit separation T, and $\omega_M(\widehat{\Psi})$ and $\Omega_N(\widehat{\Psi})$ by the slit width a." We generalize their statement: The slit width a governs $\Omega_N(\widehat{\Psi})$ and $\omega_M(\widehat{\Psi})$, while the fringe width b governs $\Omega_N(\Psi)$ and $\omega_M(\Psi)$. (For the examples we consider below, b can be identified with K_n.) Previously, the latter was governed by the slit separation T, but T is directly related to $\Omega_N(\Psi)$ and $\omega_M(\Psi)$ only in the special case considered by UH. In fact, T is a mere scaling parameter and, as would be expected, the value of the uncertainty product is independent of T. This is a straightforward consequence of the scaling property of the Fourier transform.

V. A SELECTION OF QUANTUM STATES

We are using the most common (and simplest) description of multislit experiments: A single illuminated slit is assumed to prepare a quantum state described by a rectangular function of slit width,

$$\mathrm{rec}_a(x) = \begin{cases} 1/\sqrt{a} & \text{for } x \in [-a/2, a/2], \\ 0 & \text{for } x \notin [-a/2, a/2], \end{cases} \quad (19)$$

while a general aperture mask yields a suitable superposition of those:

$$\psi(x) = \sum_j c_j\,\mathrm{rec}_a\left(x + j\frac{T}{2}\right), \quad (20)$$

where $\sum_j |c_j|^2 = 1$. Figures 2 and 3 depict examples of such wave functions. A wave function prepared through uniformly illuminating an aperture mask with four slits is displayed in Fig. 2(a). The position-space representation of such a quantum state, also referred to as the spatial wave function, is specified by

$$\psi_n(x) = \frac{1}{\sqrt{2n}}\sum_{j=1}^{n}\{\mathrm{rec}_a[x + (2j-1)T/2] + \cdots\cdots + \mathrm{rec}_a[x - (2j-1)T/2]\}. \quad (21)$$

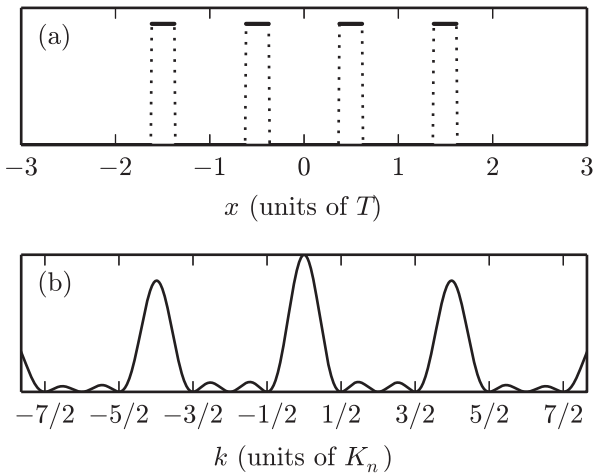

FIG. 2. The state ψ_2 is illustrated; in (a) the position-space representation $|\psi_2(x)|$ and in (b) the momentum-space representation $|\widehat{\psi}_2(k)|$. The parameters have been chosen such that $a/T = 1/4$.

The associated momentum probability distribution is depicted in Fig. 2(b). The momentum-space wave function $\widehat{\psi}_n(k)$ is given by

$$\widehat{\psi}_n(k) = \sqrt{\frac{a}{n\pi}}\,\mathrm{sinc}\left(\frac{a}{2}k\right)\sum_{j=1}^{n}\cos. \tag{22}$$

For future reference, we define

$$f_n(y) = \sum_{j=1}^{n}\cos(2j-1)y]. \tag{23}$$

Note that the central fringe of $\widehat{\psi}_n(k)$ is supported on an interval of size K_n, which thus makes a suitable measure of fringe width.

A different class of wave functions that is discussed here is depicted in Fig. 3. These quantum states provide an alternative way of producing quantum states with increasingly fine fringes by way of increasing the size of the nodes, which

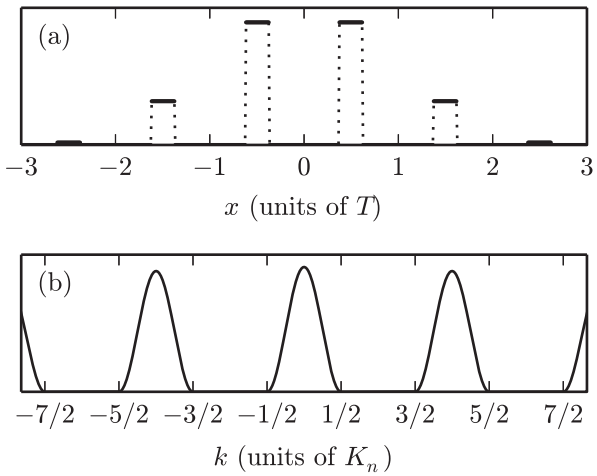

FIG. 3. The state ϕ_2 is illustrated; in (a) the position-space representation $|\phi_2(x)|$ and in (b) the momentum-space representation $|\widehat{\phi}_2(k)|$. The parameters have been chosen such that $a/T = 1/4$.

is directly related to the shape of the fringes found between two neighboring nodes. These states are specified according to

$$\phi_n(x) = [g * (\mathrm{III}_T \cdot h_n)](x), \tag{24a}$$

$$\widehat{\phi}_n(k) = [\widehat{g} \cdot (\mathrm{III}_K * \widehat{h}_n)](k). \tag{24b}$$

Throughout the present text the convolution operation is indicated using the asterisk ($*$). The Dirac comb is defined as

$$\mathrm{III}_T(x) = \sum_{j=-\infty}^{\infty}\delta(x - T/2 - jT), \tag{25}$$

$$\mathrm{III}_K(k) = \frac{\sqrt{2\pi}}{T}\sum_{j=-\infty}^{\infty}(-1)^j\delta(k - jK), \tag{26}$$

where δ denotes the delta distribution. Under Fourier transformation, the Dirac comb III_T is mapped onto a Dirac comb III_K with reciprocal spacing and a numerical factor. The function g describes the slit shape,

$$g(x) = \mathrm{rec}_a(x), \tag{27}$$

while the function $\widehat{h}_n$ is associated with the fringe shape and corresponds to

$$\widehat{h}_n(k) = \begin{cases}\sqrt{2/K_n}\cos\pi k/K_n & \text{for } k \in [-K_n/2, K_n/2],\\ 0 & \text{for } k \notin [-K_n/2, K_n/2].\end{cases} \tag{28}$$

The function $\widehat{h}_n(k)$ is supported on an interval of size K_n, which thus makes a suitable measure of fringe width.

Our parametrization is such that ϕ_1 corresponds to ψ_1 while for $d \geqslant 2$, a joint eigenfunction of commuting functions of position and momentum is obtained. These quantum states are eigenstates of periodic position and momentum projectors, which were used earlier to explain the observation of seemingly incompatible properties in Ref. [5]. They share the underlying structure with the uncertainty formulation discussed in Sec. III: These states are constructed in light of the compatibility of commuting functions of position and momentum that naturally occur in multislit experiments, whereas the uncertainty formulation addresses the incompatibility of the observables of multislit interferometry. Hence these states make natural candidates for further examination.

The quantity n expresses the "order of interference." Intuitively speaking, as n increases the quantum states feature more pronounced fringes. In the case of ϕ_n there is no particular number of illuminated slits that would serve to classify the state, because this number is in general infinity (although the intensity may be negligible in all but a small, finite number of illuminated slits). Hence we use the abstract quantity n, which is associated with the support of the principal fringe; it captures the relevant information about interference and the similarities between ψ_n and ϕ_n.

VI. UNCERTAINTY ANALYSIS PART 1

In this section we present an application of the uncertainty formulation based on the work of Aharonov *et al.* [1], to the quantum states introduced in the previous section.

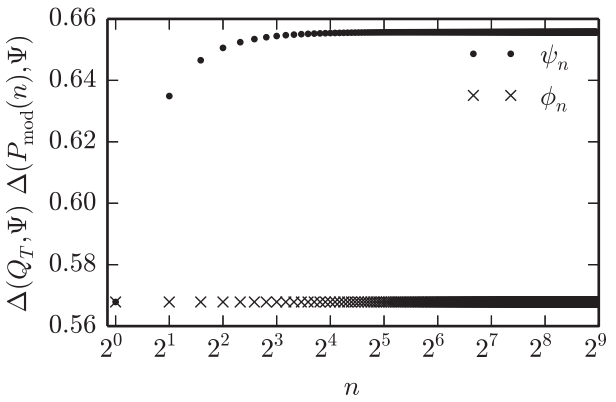

FIG. 4. The uncertainty product of Eq. (13) is illustrated for ψ_n (dots) and ϕ_n (crosses). Note that the uncertainty products coincide for $n = 1$, because $\psi_1 = \phi_1$.

A. Uncertainty of ψ_n (part 1)

In earlier work we already discussed an application of this uncertainty formulation to the states ψ_n [3]. In the interest of a self-contained exposition, we review the earlier results in preparation for further discussion below.

An expression of the standard deviation $\Delta(Q_T,\psi_n)$ is easily obtained analytically [6],

$$\Delta(Q_T,\psi_n) = T\sqrt{\frac{n^2}{3} - \frac{1}{12}}\,. \tag{29}$$

The fringe width is resolved using the operator $P_{\rm mod}(n)$ that was introduced in Eq. (11). We find

$$\begin{aligned}\Delta(P_{\rm mod}(n),\psi_n) &= \left(\frac{2}{K_n}\int_{-K_n/2}^{K_n/2} k^2\cos^2 dk\right)^{1/2}\\ &= \frac{K_n}{2\pi}\sqrt{\frac{\pi^2-6}{3}} = \frac{1}{nT}\sqrt{\frac{\pi^2-6}{3}}.\end{aligned} \tag{30}$$

Using the results of Eqs. (29) and (30), we proceed to calculate the uncertainty product for the double-slit state ψ_1 and the large-n limit. Regarding the former we find

$$\Delta(Q_T,\psi_1)\ \Delta(P_{\rm mod}(1),\psi_1) = \frac{1}{2}\sqrt{\frac{\pi^2-6}{3}}, \tag{31}$$

while for the latter we obtain

$$\begin{aligned}\lim_{n\to\infty}\Delta(Q_T,\psi_n)\ \Delta(P_{\rm mod}(n),\psi_n) &= \frac{\sqrt{\pi^2-6}}{3}\\ &\approx 0.656.\end{aligned} \tag{32}$$

We observe that this uncertainty product is smallest for the state ψ_1 and converges to a value of approximately 0.656 as n increases. This behavior of the uncertainty product is illustrated in Fig. 4. Illuminating an increasing number of slits of the aperture mask precisely reflects the change in fine structure, resulting in a converging uncertainty product.

B. Uncertainty of ϕ_n (part 1)

Calculating the standard deviation of Q_T in state ϕ_n is substantially more involved than it was for ψ_n, although the final result is rather simple. Note that the operator Q_T is sensitive only to the total probability contained in intervals of length T. Let P_j correspond to the probability in the interval $[jT,(j+1)T]$, where j is any integer. The standard deviation of Q_T in quantum state Ψ is given by

$$\Delta(Q_T,\Psi) = T\left[\sum_{j=-\infty}^{\infty} j^2\,\mathsf{P}_j - \left(\sum_{j=-\infty}^{\infty} j\,\mathsf{P}_j\right)^2\right]^{1/2}. \tag{33}$$

An aperture mask with infinitesimal slits prepares a quantum state Ψ_δ, indicated by the δ subscript. The variance of Q in state Ψ_δ is given by

$$\Delta(Q,\Psi_\delta) = T\left(\sum_{j=-\infty}^{\infty}(j+1/2)^2\,\mathsf{P}_j\right)^{1/2}. \tag{34}$$

Following from our assumption of even probability distributions, i.e., we assume that $|\psi(x)|^2 = |\psi(-x)|^2$, the two equations (33) and (34) are equal,

$$\Delta(Q_T,\psi) = \Delta(Q,\psi_\delta). \tag{35}$$

This is shown explicitly in Appendix A. While the operator Q_T is insensitive to detailed features of the probability distribution of ψ, the state ψ_δ lacks them. Note that according to Eq. (35) the spatial localization property does not depend on the shape of the slits in general.

An explicit expression for $\Delta(Q_T,\phi_n)$ can now be obtained using Eq. (35), the result of Appendix B, and $\widehat{h}_n$ as specified in Eq. (28). We find

$$\Delta(Q_T,\phi_n) = \Delta(Q,\phi_{n,\delta}) \tag{36}$$

$$= \Delta(Q,\phi_n) - a/12 \tag{37}$$

$$= nT/2. \tag{38}$$

The two subscripts of $\phi_{n,\delta}$ in Eq. (36) denote this quantum state as a joint eigenfunction prepared by an aperture mask with infinitesimal slits. Equation (37) follows by the calculation provided in Appendix B, while Eq. (38) follows from a straightforward calculation of the standard deviation of h_n.

Regarding the fine structure of $\widehat{\phi}_n(k)$, note the following: The only difference between the momentum-space wave functions of ψ_2 and ϕ_2, depicted in Figs. 2(b) and 3(b), respectively, is found in the effective envelope of $\widehat{\psi}_2$, i.e., the fact that $\widehat{\psi}_2$ possesses secondary maxima. However, we already discovered that the effective envelope does not contribute to the fine structure of a wave function. We conclude immediately that the fringe widths of ψ_n and ϕ_n should be identical. Indeed, this is what we find: $\Delta(P_{\rm mod}(n),\psi_n)$ can be calculated directly,

$$\begin{aligned}\Delta(P_{\rm mod}(n),\phi_n) &= \left[\frac{2}{K_n}\int_{-K_n/2}^{K_n/2} k^2\cos^2 dk\right]^{1/2}\\ &= \frac{K_n}{2\pi}\sqrt{\frac{\pi^2-6}{3}} = \frac{1}{nT}\sqrt{\frac{\pi^2-6}{3}}\end{aligned} \tag{39}$$

$$= \Delta(P_{\rm mod}(1),\phi_n). \tag{40}$$

The first equality follows, because (a) we assume that the fringes are supported on intervals of size K_n, and (b) $\Delta(P_{\rm mod},\phi_n)$ can be computed by considering a single interval of periodicity without the effective envelope. Note that according to Eq. (40), there is no benefit from adapting the operator $P_{\rm mod}(n)$ to the given experimental setup. The operator $P_{\rm mod}(n)$ is insensitive to the presence of extended nodes, i.e.,

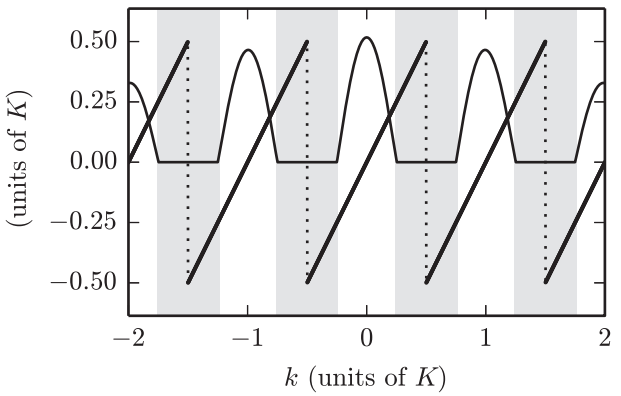

FIG. 5. The operators $P_{\mathrm{mod}}(1)$ and $|\widehat{\phi}_2(k)|^2$ are depicted. This example illustrates that for states ϕ_n the action of $P_{\mathrm{mod}}(1)$ is identical to that of $P_{\mathrm{mod}}(n)$, because only those parts of $P_{\mathrm{mod}}(1)$ contribute which are identical to $P_{\mathrm{mod}}(n)$. The other parts do not contribute, because there the wave function vanishes. In the depicted example the action of $P_{\mathrm{mod}}(1)$ is identical to that of $P_{\mathrm{mod}}(2)$. Note that the wave function, as depicted, is not normalized.

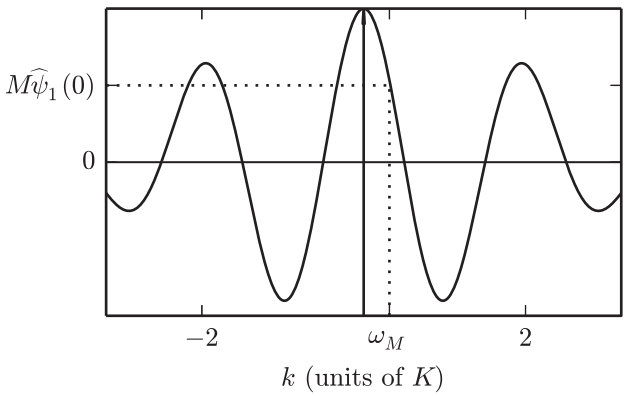

FIG. 6. An intuitive interpretation of $\omega_M(\psi)$ is illustrated here for this otherwise abstract measure. Considering a uniformly illuminated aperture mask, the mean fringe width $\omega_M(\psi)$ is equal to half the fringe width of the central peak at height $0 \leqslant M\widehat{\psi}(k) \leqslant \widehat{\psi}(k)$.

extended intervals where the wave function vanishes. See Fig. 5 for an illustration of this point.

The uncertainty product in state ϕ_n can now be calculated using Eqs. (36) and (39). We obtain

$$\Delta(Q_T,\phi_n)\,\Delta(P_{\mathrm{mod}},\phi_n) = \frac{1}{2}\sqrt{\frac{\pi^2-6}{3}}. \tag{41}$$

Evidently this formulation of uncertainty assigns the same uncertainty product to ϕ_n irrespective of the particular value of n; see Fig. 4.

VII. UNCERTAINTY ANALYSIS PART 2

In this section we investigate the uncertainty formulation due to Uffink and Hilgevoord. Any application of this formulation of uncertainty should start with choosing a suitable pair (N,M). Although Uffink and Hilgevoord discussed the mathematical constraints on (N,M)—Eqs. (17) and (18)—and argued that the precise choice is not important, we found that the results can differ: The correct choice can be made only after careful consideration of the given problem; for our purpose that is the discussion of Sec. II.

A. Uncertainty of ψ_n (part 2)

We choose $N = 1$. It follows from a simple consideration of the support property of $\psi_n(x)$ that the overall width of the given state is specified by

$$\Omega_1(\psi_n) = (2n-1)T + a\,, \tag{42}$$

featuring linear dependence on n and an absolute term a. The presence of the absolute term, however, is somewhat unwanted in the context of multislit interferometry as the slit width a is unrelated to interference. Note that its presence stems from matters of consistency: The present uncertainty formulation allows for analysis of single-slit states. Increasing the slit width to $a = T$ results in a single illuminated slit of width $mT = 2nT$, and the overall width must reflect this. Naturally, as the value of $\Omega_N(\psi_n)$ increases, this absolute term is going to become negligible.

The mean fringe width $\omega_M(\psi_n)$ can be calculated and the result is

$$\omega_M(\psi_n) = \min\left\{s : \left|\frac{1}{n}\,\mathrm{sinc}\left(\frac{a}{2}s\right) f_n\left(\frac{T}{2}s\right)\right| = M\right\}. \tag{43}$$

The function f_n was defined in Eq. (23). The derivation of Eq. (43) is provided in Appendix C, and an illustration in Fig. 6. According to Eq. (43), the mean fringe width of ψ_n depends on the slit width a. However, note the following special case:

$$\omega_0(\psi_n) = \min\left\{s : \left|\frac{1}{n}\,\mathrm{sinc}\left(\frac{a}{2}s\right) f_n\left(\frac{T}{2}s\right)\right| = 0\right\} \tag{44}$$

$$= \min\{s : \cos(2n-1)Ts/2 = 0\} \tag{45}$$

$$= \pi/(nT) = K_n/2. \tag{46}$$

When $M = 0$, the value of $\omega_0(\psi_n)$ does not depend on a, because $\omega_0(\psi_n)$ depends on the support property of the central fringe only. In fact, $\omega_0(\psi_n)$ is independent of the effective envelope, which distinguishes this particular choice of M and indicates that the desired features are captured. Noting that the sinc factor does not depend on n, the additional contributions introduced for a different choice of M are restricted to small values of n. In general, the choice of M (and N) is apparently not as straightforward as Eqs. (17) and (18) suggest. Observe that Eq. (46) simply corresponds to half the support of the central fringe.

Using Eqs. (42) and (46), we calculate the uncertainty product

$$\Omega_1(\psi_n)\,\omega_0(\psi_n) = [(2n-1)T + a]K_n/2$$

$$= 2\pi - \frac{\pi}{n} + \frac{\pi a}{nT}. \tag{47}$$

The uncertainty product decomposes naturally into three terms, each of which features different quantities and contributes depending on the respective sign. The third term depends on the ratio of slit width to slit separation (a/T) and expresses the fact that for $a = T$ any change in n would be a scale transformation without physical effect.

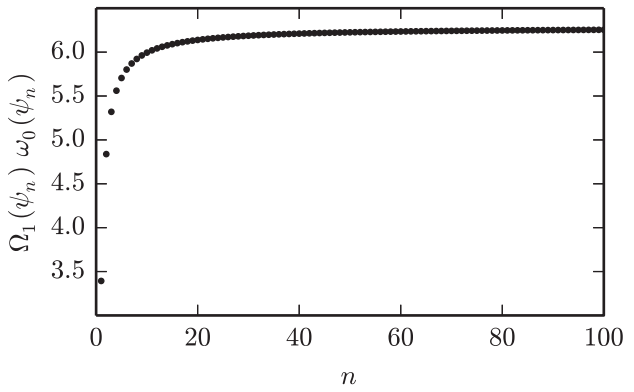

FIG. 7. Illustration of the uncertainty product given in Eq. (47) for states ψ_n. Qualitatively identical behavior is displayed as was found for APP uncertainty; compare Fig. 4.

In Fig. 7 the behavior of the uncertainty product (47) is illustrated. We observe that this uncertainty product is smallest for the state ψ_1 and converges to a value of 2π as n increases. The uncertainty product for ψ_1 would reach the lower bound in the limit of vanishing a/T.

B. Uncertainty of ϕ_n (part 2)

The states ϕ_n have the property that the associated fringes are isolated for $n \geqslant 2$; see Fig. 3. This implies that for $n \geqslant 2$ the mean fringe width $\omega_M(\phi_n)$ depends only on the overlap of a single fringe with a shifted copy. While for $n = 1$ we find the same mean fringe width as we did for ψ_1, because $\phi_1 = \psi_1$, for $n \geqslant 2$ we use Eq. (28) and obtain

$$\omega_M(\phi_n) = \min\left\{ s : \left| \operatorname{sinc}\left(\frac{a}{2}s\right)\left[\left(1 - \frac{s}{K_n}\right)\cos\pi\frac{s}{K_n} + \cdots\cdots + \frac{1}{\pi}\sin\pi\frac{s}{K_n}\right]\right| = M \right\}. \tag{48}$$

The calculation leading to this result is provided in Appendix D. The min condition requires that $s \leqslant K_n$. Hence, assuming $s \leqslant K_n$ enables us to simplify the entire expression:

$$M = \operatorname{sinc}\left(\frac{a}{2}\omega_M(\phi_n)\right)\left[\left(1 - \frac{\omega_M(\phi_n)}{K_n}\right)\cos\pi\frac{\omega_M(\phi_n)}{K_n} + \cdots\cdots + \frac{1}{\pi}\sin\pi\frac{\omega_M(\phi_n)}{K_n}\right] \tag{49}$$

It follows immediately from this result that $\omega_M(\phi_n)$ must be directly proportional to K_n for M to remain approximately constant across n (accurate for $a/T \to 0$). Just as for the previously investigated ψ_n, Eq. (43), we find a dependence on a. For $a \ll T$ this dependence becomes negligible numerically, and we ignore it under this assumption henceforth. We set

$$\omega_M(\phi_n) = c_M\, K_n. \tag{50}$$

The non-negative number c_M determines the particular value of M; c_M is necessarily smaller than or equal to unity. For the states ψ_n we found a similar expression in Eq. (46) and conclude $\omega_M(\phi_n) \propto \omega_M(\psi_n)$. We make the arbitrary choice $c_M = 1/2$, which results in $M = 1/\pi$ and gives

$$\omega_{\pi^{-1}}(\phi_n) = K_n/2 = \pi/(nT). \tag{51}$$

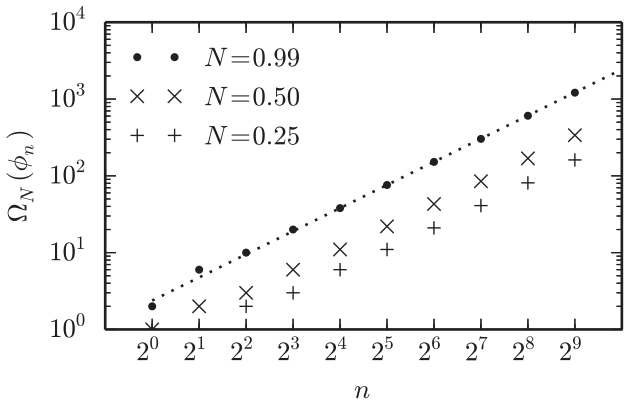

FIG. 8. The scaling of the overall width in state ϕ_n is depicted for three choices of N. The numerical calculations show that asymptotically $\Omega_N(\phi_n)$ depends linearly on n. The dotted line corresponds to Eq. (55). Observe that $N = 0.25$ and $N = 0.5$ do not make suitable choices according to Eqs. (17) and (18), but are represented in order to illustrate the mathematical aspects of the overall width.

Regarding the overall width $\Omega_N(\phi_n)$, not much can be said in terms of analytical results. While it is fairly simple to show that $\Omega_N(\phi_n)$ is approximately proportional to n, more concrete results are difficult to obtain. The proportionality follows from a straightforward calculation of the function determining the overall width,

$$h_n(x) = \frac{1}{\sqrt{2\pi}}\int_{-K_n/2}^{K_n/2}\sqrt{\frac{2}{K_n}}\cos e^{ixk}dk, \tag{52}$$

$$= H(K_n x). \tag{53}$$

The argument of the function H scales inversely with n, which means that $\Omega_N(\phi_n)$ will approximately scale with n. Our numerical investigation shows that $\Omega_N(\phi_n)$ indeed displays this behavior in the limit of large n. See Fig. 8, which depicts identical qualitative behavior for three different choices of N. We conclude that

$$\Omega_N(\phi_n) = \pi c_N T n \quad \text{for large } n. \tag{54}$$

The linear dependence on T follows from the general discussion in Sec. IV. The numerical factor c_N is non-negative, but otherwise undetermined. Explicit values of c_N are not obtained as easily as for c_M. We approximate the value of c_N using numerical investigations. For example, inspection of the data points in Fig. 8 suggests

$$\Omega_{0.99}(\phi_n) \approx 2^{1.25} T n, \tag{55}$$

indicated by the dotted line displayed in Fig. 8. Using this expression along with the result for $\omega_{\pi^{-1}}(\phi_n)$ in Eq. (51), we calculate the asymptotic behavior of the uncertainty product for the given choices of N and M. We find that asymptotically a precise tradeoff occurs:

$$\Omega_{0.99}(\phi_n)\,\omega_{\pi^{-1}}(\phi_n) \approx 7.47 \quad \text{for large } n. \tag{56}$$

The convergence of this particular uncertainty product is illustrated in Fig. 9, showing that the uncertainty product converges to a value of approximately 7.41. This is in good agreement with our prediction, which was based solely on inspection of the data points of Fig. 8.

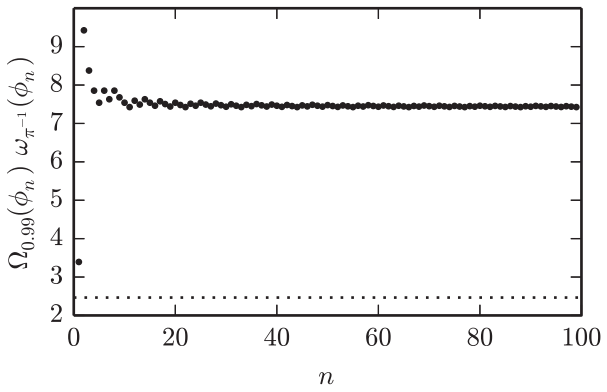

FIG. 9. Illustration of the uncertainty product given in Eq. (56) for states ϕ_n. The dotted line represents the lower bound on the uncertainty product. Compare Fig. 4, which illustrates the qualitatively similar behavior of the uncertainty product (13) for large values of n.

A different choice of a/T would allow for ϕ_1 to reach the lower bound, which is illustrated in Fig. 9 by the dotted line. It is unclear, however, whether the asymptotic limit or a particular uncertainty product could be decreased to meet the lower bound.

A general expression for the uncertainty product is obtained from Eqs. (50) and (54),

$$\Omega_N(\phi_n)\,\omega_M(\phi_n) \approx 2\pi_N c_M \quad \text{for large } n\,. \tag{57}$$

This is the general form of the asymptotic limit of the uncertainty product for the states ϕ_n. It remains approximately true for small values of n, but no definite statement can be made due to the discrete character of the measures used. It is, in fact, this discreteness that results in the erratic behavior of the uncertainty product for small values of n.

VIII. COMPARISON AND CONCLUSION

We now compare the results of our example applications and discuss the similarities and differences between the two uncertainty formulations. We also address to what extent the general considerations are met that were discussed in Sec. II.

The applications presented here show that both uncertainty formulations yield qualitatively similar results. This is reassuring, independently confirming that the relevant physical structure is captured. However, it is not necessarily straightforward to arrive at this conclusion in general terms, because the two uncertainty formulations appear to be very different. In actual fact, although implemented differently, the respective measures describe very similar observables. In particular, both uncertainty formulations feature measures that relate to the width of the fringes. This captures the relevant observable in accordance with the discussion of Sec. II. The particular measures employed, though, are rather different. The formulation based on Aharonov *et al.* employs a measure that corresponds to computing the standard deviation of a single fringe while neglecting the effective envelope. The formulation due to Uffink and Hilgevoord is based on the autocorrelation function of the interference wave function, and in general features a (possibly negligible) dependence on the fundamental envelope.

The analysis of the quantum states ψ_n, prepared through uniform illumination of an aperture mask, resulted in qualitatively identical results. Figures 4 and 6 show that both uncertainty products display the same behavior: Starting at a minimal uncertainty product for ψ_1, the uncertainty product converges to some larger, finite value as n increases. However, the uncertainty formulation due to Uffink and Hilgevoord actually allows for the lower bound to be reached in the limit of vanishing slit width. This noncritical dependence on the slit width is actually somewhat unwanted for purely multislit considerations. The measures used in the uncertainty formulation based on Aharonov *et al.* do not depend on the slit width or the related envelope function of the interference pattern.

The second example application involves quantum states ϕ_n, which are characterized by their extended nodes. In this case, for the uncertainty formulation based on Aharonov *et al.* the uncertainty tradeoff is exact and the uncertainty product constant across n. For the formulation of uncertainty due to Uffink and Hilgevoord this is the case only in the limit of large n, because of the discrete quality of the employed measures. See Figs. 4 and 9. Also note that the measure of fringe width employed by Uffink and Hilgevoord results in a dependence on the slit width. For most considerations this dependence may be negligible with regard to numerical results, but poses a qualitative difference. In general, a dependence on the particular aperture is to be expected for this uncertainty formulation, although in some cases a particular parameter choice may remove this dependence (as is the case for ψ_n).

Regarding technical aspects, we found that the formulation of uncertainty due to Uffink and Hilgevoord is computationally more difficult. For our second example application we resorted to numerical analysis in order to obtain an approximate expression for the spatial localisation. (The formulation based on the work of Aharonov *et al.* was not particularly straightforward to apply to this scenario either, but a satisfying analytical result was obtained eventually.) This is further complicated by the two degrees of freedom N and M. Uffink and Hilgevoord found that the exact choice of N and M is not important to the analysis of single- or double-slit experiments—while adhering to the conditions (17) and (18), of course. In the context of multislit experiments, however, we found that additional insight may be required for appropriately choosing (N,M).

ACKNOWLEDGMENTS

The author would like to thank P. Busch (University of York) for valuable discussions at various stages of the investigation and for his suggestions regarding its final presentation. The author would also like to thank P. J. Coles (University of Singapore) for fruitful discussions during the Central European Workshop on Quantum Optics 2014, which helped shape this manuscript.

APPENDIX A

Here we show the validity of Eq. (35). In order to establish the claim, we proceed to show that

$$\sum_{i=-\infty}^{\infty} i^2 \mathsf{P}_j - \left(\sum_{i=-\infty}^{\infty} i\mathsf{P}_j\right)^2 = \sum_{i=-\infty}^{\infty} (i+1)^2 \mathsf{P}_j, \tag{A1}$$

using the following two results:

$$\sum_{i=-\infty}^{\infty} i\mathsf{P}_j = \sum_{i=-\infty}^{-1} i\mathsf{P}_j + \sum_{i=0}^{\infty} i\mathsf{P}_j \tag{A2}$$

$$= \sum_{i=1}^{\infty} (-i)\mathsf{P}_{i-1} + \sum_{i=0}^{\infty} i\mathsf{P}_j \tag{A3}$$

$$= -\sum_{j=0}^{\infty} (j+1)\mathsf{P}_j + \sum_{i=0}^{\infty} i\mathsf{P}_j \tag{A4}$$

$$= \sum_{i=0}^{\infty} [i-(i+1)]\mathsf{P}_i = -\frac{1}{2}. \tag{A5}$$

This result is obtained using the symmetry of the probability distribution, i.e., $|\psi(x)| = |\psi(-x)|$, which entails $\mathsf{P}_j = \mathsf{P}_{-i-1}$. A very similar calculation yields

$$\sum_{i=-\infty}^{\infty} i^2\mathsf{P}_j = 2\sum_{i=0}^{\infty} i^2\mathsf{P}_j - \frac{1}{2}. \tag{A6}$$

Hence the left-hand side of (A1) becomes

$$\sum_{i=-\infty}^{\infty} i^2\mathsf{P}_j - \left(\sum_{i=-\infty}^{\infty} i\mathsf{P}_j\right)^2 = 2\sum_{i=0}^{\infty} i^2\mathsf{P}_j - \frac{3}{4}, \tag{A7}$$

whereas the right-hand side of (A1) becomes

$$\sum_{i=-\infty}^{\infty} (i+1)^2\mathsf{P}_j = 2\sum_{i=0}^{\infty} i^2\mathsf{P}_j - \frac{1}{2} + \left(\frac{-1}{2}\right)^2 + \frac{1}{4} \tag{A8}$$

$$= 2\sum_{i=0}^{\infty} i^2\mathsf{P}_j - \frac{3}{4}. \tag{A9}$$

This shows the claimed proportionality of Eqs. (33) and (34). Note that we assume nothing about the illumination of the aperture, only that it be symmetrical about the origin.

APPENDIX B

Here we show how Eq. (37) is obtained. We denote the limits of integration using $\alpha = jT - a/2$ and $\beta = jT + a/2$.

$$\Delta(Q,\Psi) = \sum_{j=1}^{m}\int_{\alpha}^{\beta} \frac{x^2\mathsf{P}_j}{a}dx - \left(\sum_{j=1}^{m}\int_{\alpha}^{\beta} \frac{x\,\mathsf{P}_j}{a}dx\right)^2$$

$$= \sum_{j=1}^{m}\mathsf{P}_j\int_{\alpha}^{\beta} \frac{x^2}{a}dx - \left(\sum_{j=1}^{m}\mathsf{P}_j\int_{\alpha}^{\beta} \frac{x}{a}dx\right)^2 \tag{B1}$$

$$= \sum_{j=1}^{m}\mathsf{P}_j\left(\frac{a}{12} + j^2T^2\right) - \left(\sum_{j=1}^{m}\mathsf{P}_j jT\right)^2 \tag{B2}$$

$$= \sum_{j=1}^{m}\mathsf{P}_j\frac{a}{12} + \sum_{j=1}^{m}\mathsf{P}_j j^2T^2 - \left(\sum_{j=1}^{m}\mathsf{P}_j jT\right)^2. \tag{B3}$$

Here we use the fact that the probabilities P_j sum to unity in order to simplify the first term. We obtain

$$= \frac{a}{12} + \sum_{j=1}^{m}\mathsf{P}_j j^2T^2 - \left(\sum_{j=1}^{m}\mathsf{P}_j jT\right)^2 \tag{B4}$$

$$= \frac{a}{12} + \Delta(Q,\Psi_\delta), \tag{B5}$$

which is the desired result.

APPENDIX C

The derivation of the mean peak width in state ψ_n, Eq. (43), is provided here. We proceed to calculate the autocorrelation function of $\psi_n(x)$.

$$\int_{-\infty}^{\infty} \widehat{\psi}_n(k)\widehat{\psi}_n(k-s)dk$$

$$= \frac{2a}{nT\pi}\int \mathrm{sinc}\left(\frac{a\kappa}{T}\right)\mathrm{sinc}\left(\frac{a}{T}(\kappa-s)\right) f_n(\kappa)f_n(\kappa-s)d\kappa, \tag{C1}$$

where we are using the shorthand $f_n(k)$, which was introduced in Eq. (23), and the dimensionless variable $\kappa = Tk/2$. This integral may be decomposed into an infinite sum of integrals over the finite interval K ($= \pi$ in units of κ),

$$= \frac{2a}{nT\pi}\sum_{j=-\infty}^{\infty}\int_{(j-1/2)\pi}^{(j+1/2)\pi} \mathrm{sinc}\left(\frac{a}{T}\kappa\right)\mathrm{sinc}\left(\frac{a}{T}(\kappa-s)\right)$$

$$\times \cdots\cdots \times f_n(\kappa)f_n(\kappa-s)d\kappa. \tag{C2}$$

We now substitute $u = \kappa - j\pi$ and immediately exploit the periodicity of f_n, i.e., that $f_n(\kappa + j\pi)^2 = f_n(\kappa)^2$,

$$= \frac{2a}{nT\pi}\sum_{j=-\infty}^{\infty}\int_{-\pi/2}^{\pi/2} \mathrm{sinc}\left(\frac{a}{T}(u+j\pi)\right)$$

$$\times \mathrm{sinc}\left(\frac{a}{T}(u+j\pi-s)\right) f_n(u)f_n(u-s)du \tag{C3}$$

$$= \frac{2a}{nT\pi}\int_{-\pi/2}^{\pi/2}\left[\sum_{j=-\infty}^{\infty} \mathrm{sinc}\left(\frac{a}{T}(u+j\pi)\right)\right.$$

$$\left.\times \mathrm{sinc}\left(\frac{a}{T}(u+j\pi-s)\right)\right] f_n(u)f_n(u-s)du. \tag{C4}$$

The sum in square brackets can be evaluated by means of a general result adapted to the particular problem: According to Eq. (11) of Ref. [7] and the derivation provided in Ref. [8],

$$\sum_{j=-\infty}^{\infty} \mathrm{sinc}(\alpha\,(v+j))\,\mathrm{sinc}(\alpha(w+j)) \tag{C5}$$

$$= \int_{-\infty}^{\infty} \mathrm{sinc}[\alpha(v+x)]\,\mathrm{sinc}[\alpha(w+x)]dx \tag{C6}$$

$$= \frac{\pi}{\alpha}\,\mathrm{sinc}[\alpha(v+w)]. \tag{C7}$$

The integration of the penultimate line can be evaluated to yield the final expression. Using the definitions

$$v = u/\pi, \quad w = (u-s)/\pi, \quad \alpha = a\pi/T, \tag{C8}$$

we return to the expression to be evaluated and obtain

$$= \frac{2a}{nT\pi}\frac{T}{a}\mathrm{sinc}\left(\frac{a}{T}s\right)\int_{-\pi/2}^{\pi/2} f_n(u)f_n(u-s)du \tag{C9}$$

$$= \frac{2}{n\pi}\mathrm{sinc}\left(\frac{a}{T}s\right)\int_{-\pi/2}^{\pi/2} f_n(u)f_n(u-s)du \tag{C10}$$

$$= \frac{2}{n\pi}\mathrm{sinc}\left(\frac{a}{T}s\right)\frac{\pi}{2}f_n(s) = \frac{1}{n}\mathrm{sinc}\left(\frac{a}{T}s\right)f_n(s). \tag{C11}$$

The desired expression now follows trivially by means of Eq. (15). Note that when $f_n(s) = 0$, there is no dependence on a. In regular units (k) this is the case for $s = \pi/nT$.

APPENDIX D

The calculation of $\omega_M(\phi_n)$, Eq. (48), proceeds identically to the calculation provided in Appendix C, the only difference being that instead of f_n we consider H_n,

$$H_n(k) = \sum_{j=-\infty}^{\infty} \widehat{h}_n(k - jK). \tag{D1}$$

For $n \geqslant 2$, we calculate the autocorrelation function of $\widehat{\phi}_n(k)$,

$$\int_{-\infty}^{\infty} \widehat{\phi}_n(k)\widehat{\phi}_n(k-s)dk \tag{D2}$$

$$= \frac{2an}{\pi}\int \mathrm{sinc}\left(\frac{ak}{2}\right)\mathrm{sinc}\left(\frac{a}{2}(k-s)\right)H_n(k)H_n(k-s)dk.$$

(All normalization factors are removed from the integral, including those of H_n.) As previously, this integral may be decomposed into an infinite sum of integrals over the finite interval K. Upon substituting $u = k - jK$, the periodicity of H_n can be exploited, and the sum over the two sinc functions evaluated. We arrive at

$$= \frac{2an}{\pi}\frac{T}{a}\mathrm{sinc}\left(\frac{a\pi}{T}\frac{s}{K}\right)\int_{-K/2}^{K/2} H_n(u)H_n(u-s)du \tag{D3}$$

$$= \frac{2nT}{\pi}\mathrm{sinc}\left(\frac{a}{2}s\right)\int_{-K_n/2}^{K_n/2} H_n(u)H_n(u-s)du \tag{D4}$$

$$= \frac{1}{\pi}\mathrm{sinc}\left(\frac{a}{2}s\right)\left[\left(\pi - n\frac{T}{2}s\right)\cos n\frac{T}{2}s + \sin n\frac{T}{2}s\right] \tag{D5}$$

$$= \mathrm{sinc}\left(\frac{a}{2}s\right)\left[\left(1 - \frac{s}{K_n}\right)\cos\pi\frac{s}{K_n} + \frac{1}{\pi}\sin\pi\frac{s}{K_n}\right]. \tag{D6}$$

This is the desired expression. The suppressed detail of this calculation is provided in Ref. [9].

[1] Y. Aharonov, H. Pendleton, and A. Peterson, Int. J. Theor. Phys. **2**, 213 (1969).

[2] J. B. M. Uffink and J. Hilgevoord, Found. Phys. **15**, 925 (1985).

[3] J. C. G. Biniok, P. Busch, and J. Kiukas, Phys. Rev. A **90**, 022115 (2014).

[4] H. J. Landau and H. O. Pollak, Bell Syst. Tech. J. **40**, 65 (1961).

[5] J. C. G. Biniok and P. Busch, Phys. Rev. A **87**, 062116 (2013).

[6] C. Gneiting and K. Hornberger, Phys. Rev. Lett. **106**, 210501 (2011).

[7] A. B. Bhatia and H. Krishnan, Proc. R. Soc. London **192**, 181 (1948).

[8] R. P. Boas, Jr. and H. Pollard, Am. Math. Monthly **80**, 18 (1973).

[9] J. C. G. Biniok, Ph.D. thesis, University of York, 2014.